

# Electric-Field-Driven Accumulation and Alignment of CdSe and CdTe Nanorods in Nanoscale Devices

Zonghai Hu,<sup>†</sup> Michael D. Fischbein,<sup>†</sup> Claudia Querner, and Marija Drndić\*

*Department of Physics and Astronomy, University of Pennsylvania, 209 South 33rd Street, Philadelphia, Pennsylvania 19104*

*Received August 29, 2006; Revised Manuscript Received October 3, 2006*

## ABSTRACT

Local electric fields generated by nanopatterned electrodes were used to control the position and orientation of well-isolated as well as closely packed colloidal semiconducting CdTe and CdSe nanorods (NRs) drop-cast from solution. Postdeposition imaging using transmission-electron microscopy and atomic-force microscopy revealed strong NR alignment to the direction of the applied field and dense accumulation around and onto voltage-biased electrodes when deposited from dilute and concentrated solutions, respectively. The degree of alignment under the applied electric field is characterized by a nematic order parameter  $S \approx 0.8$  in contrast to the zero-field case when  $S \approx 0.1$ .

Nanocrystals (NCs) are promising building blocks for functional materials and integrated devices because of their size- and shape-dependent properties.<sup>1</sup> Spherical NCs can self-assemble on a substrate into large hexagonally close-packed superlattices<sup>2–4</sup> and elongated NCs, that is, nanorods (NRs), can form liquid-crystal phases.<sup>5,6</sup> The ability to control the position and arrangement of NCs inside of a device is desirable both scientifically and technologically. Spherical NCs have been electrostatically trapped in small electrode gaps,<sup>7</sup> collected in large numbers onto electrodes by electrodeposition,<sup>8</sup> and trapped into lithographically patterned trenches on SiO<sub>2</sub> substrates by capillary forces.<sup>9</sup>

In contrast to spherical NCs, NRs have an aspect ratio  $> 1$ , and control of their angular orientation is necessary to achieve complete positional specificity. In particular, aligning individual NRs to a preferred axis is interesting for studies of single-NR luminescence and for applications in optoelectronics because NRs emit linearly polarized light along their long axis.<sup>10</sup>

CdSe and CdS NRs have been observed to collectively self-assemble into liquid-crystal patterns.<sup>5,6</sup> When deposited from slowly evaporating solutions, superlattices can form with the NRs perpendicular to the surface of the substrate.<sup>5</sup> Such superlattices can become larger in the presence of a global electric field,<sup>11,12</sup> suggesting that mechanisms such as charge and/or dipole interactions exist and contribute to NR self-assembly. In fact, CdS NRs were recently reported

to self-assemble head-to-tail into long stripe patterns,<sup>13</sup> indicative of dipole interactions. The significant role of charge in self-assembly has already been demonstrated for the case of spherical NCs.<sup>3</sup> The existence of a charge and/or dipole moment in NRs may be exploited for controlled assembly and is also interesting from a fundamental science point of view.

Attempts to directly detect the presence of charge and dipole moment in NRs have yielded a range of seemingly contradictory results. Electrostatic force microscopy (EFM) performed on CdSe NRs on HOPG substrates revealed a static charge but no dipole moment.<sup>14</sup> Absorption spectroscopy of CdSe NRs in solution with an applied electric field suggested the presence of a large dipole moment but no accumulation of the NRs onto the electrodes, implying that they have no charge.<sup>15</sup> The details of NR synthesis, the NR crystal structure, and the specific environment around the NRs as well as other factors might all affect these physical quantities. More studies are therefore needed to determine the existence and origin of charge and dipole moments in semiconducting NRs.

In this Letter, we report for the first time the alignment of CdSe and CdTe NRs to applied electric fields and their accumulation onto voltage-biased electrodes and within the gap between the electrodes after drop-casting from solution. To study the response of NRs to applied electric fields, we fabricated devices consisting of electrode gaps patterned by electron beam lithography (EBL) on  $\sim 100$ -nm-thick silicon nitride (Si<sub>3</sub>N<sub>4</sub>) suspended membranes. Using a thin suspended membrane as a substrate allowed for high-resolution imaging

\* To whom correspondence should be addressed: E-mail: drndic@physics.upenn.edu; phone: (215) 898-5810; fax: (215) 898-2010.

<sup>†</sup> These authors contributed equally to this work.

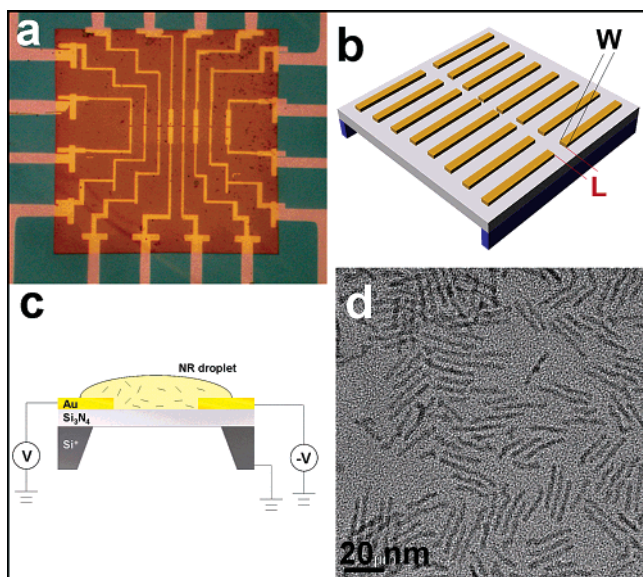


**Figure 1.** (a) Optical micrograph of a typical device containing eight electrode pairs on a  $80 \times 80 \mu\text{m}^2$   $\text{Si}_3\text{N}_4$  membrane window (copper-colored square). (b) Schematic of a device showing the suspended membrane containing eight patterned electrode pairs with different gap widths  $W$  ( $0.5\text{--}20 \mu\text{m}$ ) and lengths  $L$  ( $0.1\text{--}1.1 \mu\text{m}$ ). (c) Schematic of the experiment: voltage is applied to the electrodes, while a drop of solution containing NRs dries on the surface. The p-doped Si layer is grounded. (d) TEM image of randomly oriented  $38 \text{ nm} \times 3.4 \text{ nm}$  CdSe NRs, used in this study, imaged on a holey carbon grid.

of the devices and their content with transmission electron microscopy (TEM).<sup>16</sup> Figure 1a shows an optical micrograph of a typical device used in this study. As shown, the device consists of eight electrode pairs with capacitor plate geometry. By varying the gap lengths on a single device, a variety of electric fields could be generated with a single voltage source. The gap dimensions were varied from  $L = 0.1$  to  $1.1 \mu\text{m}$  and  $W = 0.5$  to  $15 \mu\text{m}$  (Figure 1b). Nanoscale devices allow the application of high electric fields ( $\sim 10^8 \text{ V/m}$ ), which is impractical with macroscopic electrodes because of the high voltages required to obtain the same fields.

We studied  $3.4 \text{ nm} \times 38 \text{ nm}$  TOPO-capped CdSe NRs (Figure 1d) and  $6 \text{ nm} \times 50 \text{ nm}$  TOPO-capped CdTe NRs,<sup>17</sup> prepared using the multiple-injection method.<sup>18</sup> CdSe or CdTe NRs ( $10 \mu\text{L}$ ) in a hexane/octane solution were drop-cast onto each device while voltage was applied to the electrodes. The NR solution concentration was varied from  $1 \times 10^{12}$  to  $1 \times 10^{14}$  rods/mL in order to explore the NR response to the applied field in the limit of weak (diluted solutions) and strong (moderately concentrated solutions) NR–NR interactions. Applied voltages were varied from  $\pm 5$  to  $\pm 10 \text{ V}$  because the electrode gaps became unstable for larger voltages. Some electrode gaps were biased during drop-casting while the rest were left floating in order to facilitate control studies. The p-doped Si substrate was grounded in all experiments. Drop-casting was done in  $\text{N}_2$  atmosphere, directly inside a small atomic force microscope (AFM) chamber [Veeco EnviroScope (Figure 1c)]. After an initial drying period in  $\text{N}_2$ , which was varied from several minutes to several hours, the AFM chamber pressure was

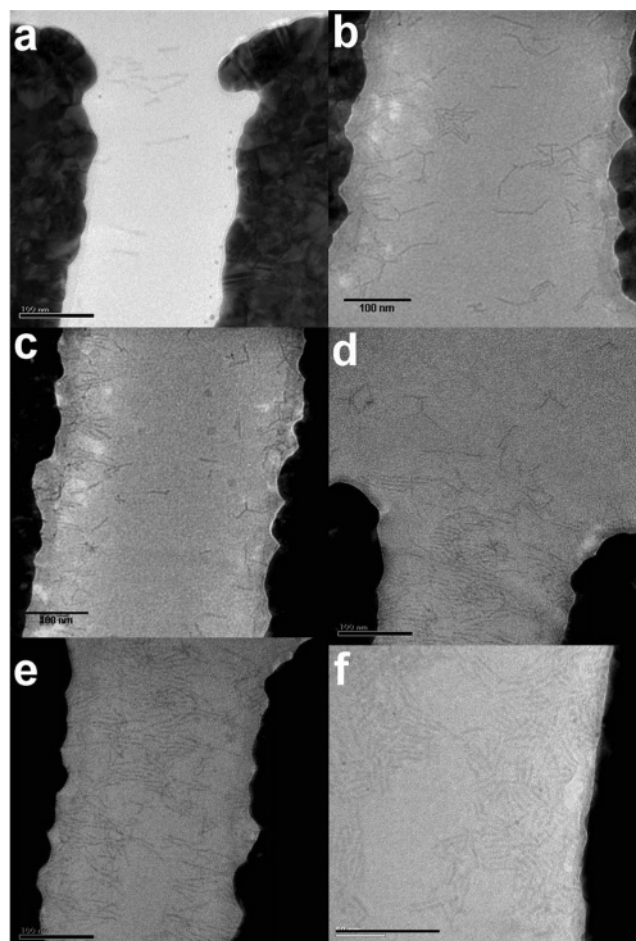


**Figure 2.** TEM images of electric field ( $E$ ) driven alignment of NRs drop-cast from dilute hexane/octane solutions on five different gaps. (a) CdTe NRs ( $\sim 10^{12}$  rods/mL;  $E = 2.8 \times 10^7 \text{ V/m}$ ). (b and c) CdSe NRs ( $\sim 10^{12}$  rods/mL;  $E_b = 1.6 \times 10^7 \text{ V/m}$  and  $E_c = 1.8 \times 10^7 \text{ V/m}$ , respectively). (d and e) CdSe NRs are close enough to show a contribution of NR–NR interaction to the predominantly electric field ( $\sim 10^{13}$  rods/mL;  $E = 2.4 \times 10^7 \text{ V/m}$ ) driven assembly. (f) Control measurement ( $\sim 10^{14}$  rods/mL;  $E = 0 \text{ V/m}$ ) showing randomly oriented CdSe NRs. All scale bars =  $100 \text{ nm}$ .

reduced to  $\sim 10^{-5}$  Torr and the drying was allowed to continue for several more hours. Postdeposition, the NRs were imaged with both AFM and TEM. A total of 25 devices were studied this way.

Figure 2a is a TEM image showing the result of CdTe NR deposition from a dilute solution ( $\sim 10^{12}$  rods/mL) onto a device with the left and right electrodes biased at 5 and  $-5 \text{ V}$ , respectively. The electric field inside the gap is  $E = V/(\epsilon L) = 2.8 \times 10^7 \text{ V/m}$ , where  $\epsilon$  is the dielectric constant of the solvent ( $\epsilon \approx 2$ ) and  $L$  is the gap length. Figure 2b and c shows results for CdSe NRs under similar conditions (concentration  $\sim 10^{12}$  rods/mL and bias  $\pm 6 \text{ V}$ ). The NRs are predominantly oriented parallel to the applied electric field (i.e., perpendicular to the faces of the electrodes). At this concentration, the NRs are well-separated (average distance  $\approx 20 \text{ nm}$ ) and their orientation is therefore the result of the applied field. For slightly higher concentrations ( $\sim 10^{13}$  rods/mL) the NRs interact with close neighbors and most likely assist each other in aligning to the field direction (Figure 2d and e). Figure 3 shows the complete  $200 \text{ nm} \times$

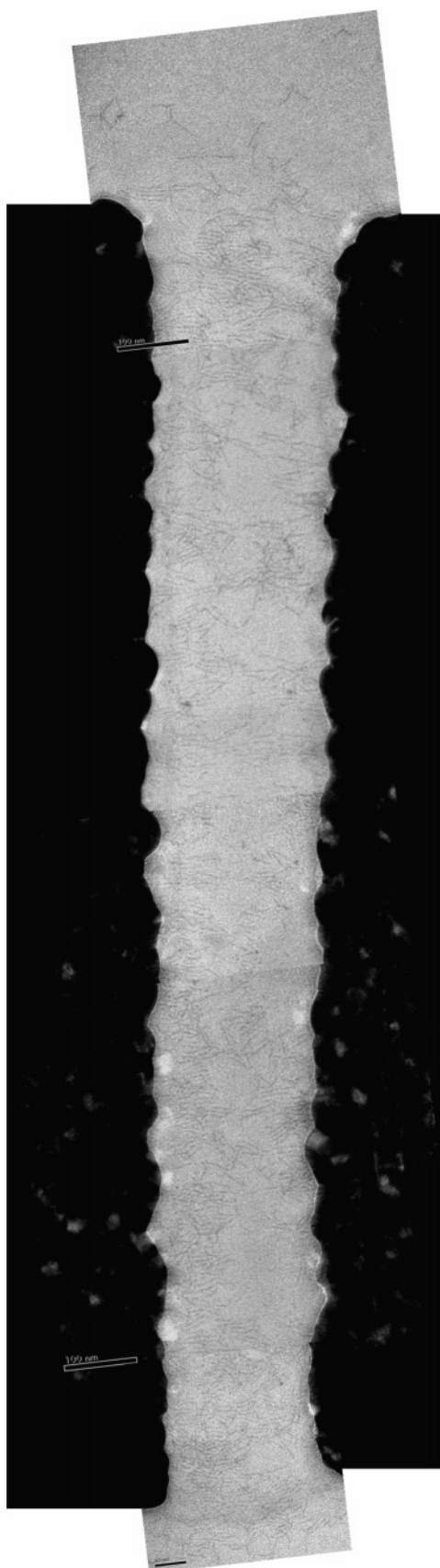


**Figure 3.** TEM image (created by pasting together six high-magnification TEM images) of a complete electrode gap ( $L = 250$  nm,  $W = 2 \mu\text{m}$ ) after deposition of a dilute solution ( $\sim 10^{13}$  rods/mL) of CdSe NRs at  $E = 2.4 \times 10^7$  V/m. The order parameter for this gap was determined to be  $S = 0.83$  (cf. Supporting Information Figure S2).

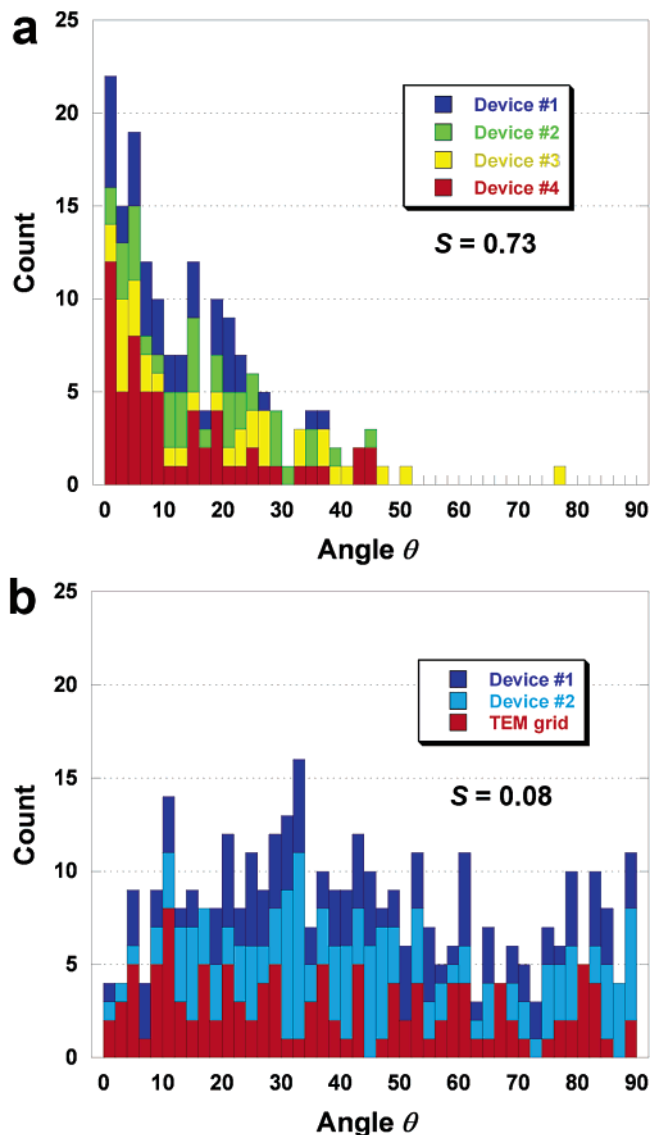


**Figure 4.** Order parameter analysis of CdSe NR alignment from dilute solution (a) at  $E \approx 2 \times 10^7$  V/m including 4 different electrode gaps with a total of 172 rods (39, 39, 34, and 60 NRs, respectively) giving an average order parameter of  $S = 0.73$  (0.86, 0.65, 0.77, and 0.83, respectively) and (b) at zero-field in 2 electrode gaps and on a TEM grid, making a total of 366 rods (112, 134, and 120 NRs, respectively) giving an average order parameter of 0.08 (0.05, 0.02, and 0.16, respectively). The bin size is  $2^\circ$ . The order parameter appears independent from the concentration in this range.

$2 \mu\text{m}$  gap introduced in Figure 2d and e. In the case of zero electric field (Figure 2f) the azimuthal orientations of NRs appear random.

To quantify the degree of NR alignment in the electrode gaps, we used a nematic order parameter defined as  $S = \langle 2 \cos^2 \theta - 1 \rangle_\theta$ . Here,  $\theta$  is the angle of a single NR relative to the direction of the electric field and  $S$  is an average over all NRs in a given electrode gap. This expression, accounting for the two-dimensional nature of the NR alignment in the plane of the substrate, is a convenient choice because, after averaging,  $S = 1$  for perfect alignment and  $S = 0$  for completely random orientations. For each device, the corresponding TEM images were analyzed with

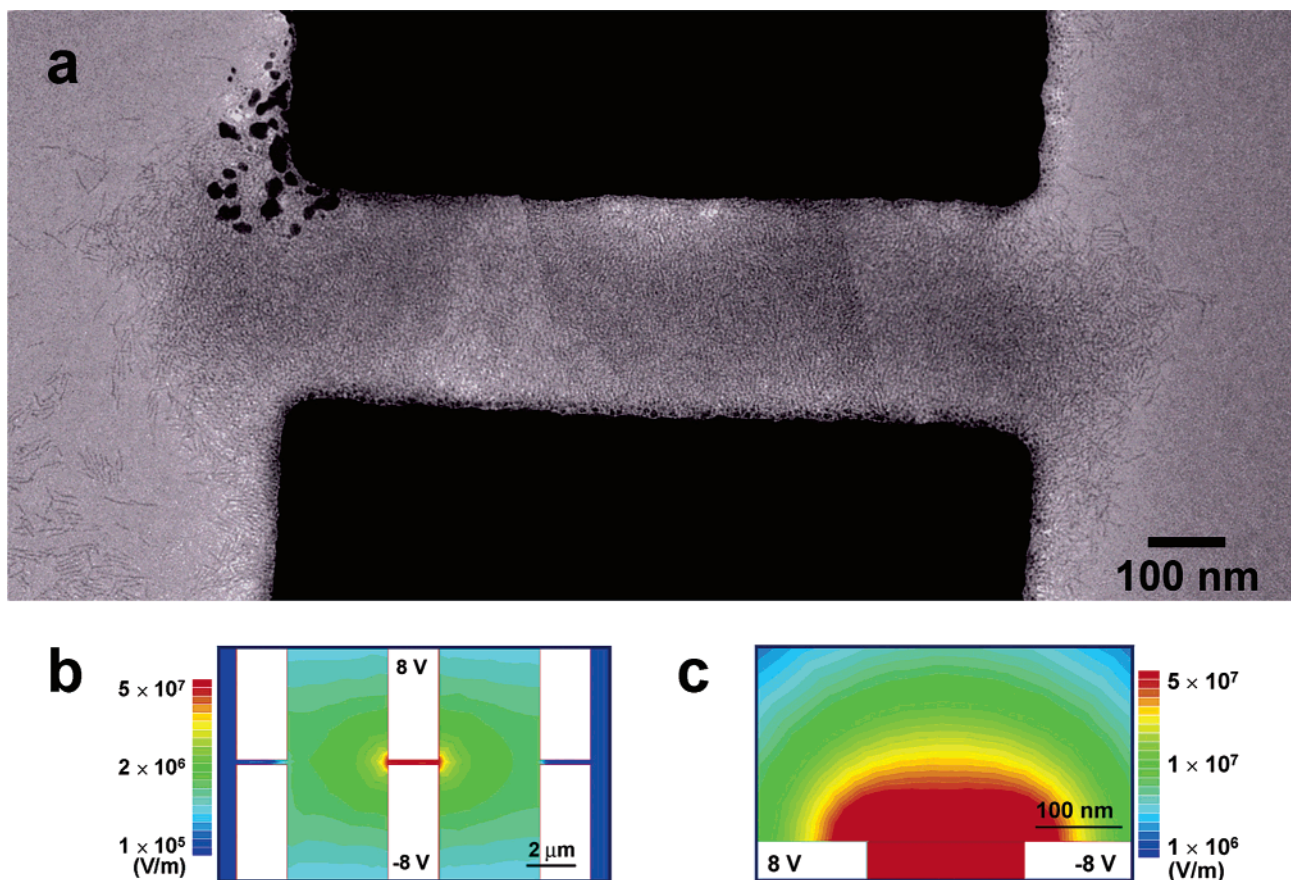


**Figure 5.** TEM image (created by pasting together three images) of an electrode gap ( $L = 270$  nm,  $W = 1$   $\mu\text{m}$ ) after deposition of CdSe NRs ( $\sim 5 \times 10^{13}$  rods/mL,  $E = 3.0 \times 10^7$  V/m). (a) Overview image of the NRs localized in the gap. (b and c) Maxwell 2D simulations in the  $x$ - $y$  plane (b) and in the  $x$ - $z$  plane (c) of the device.

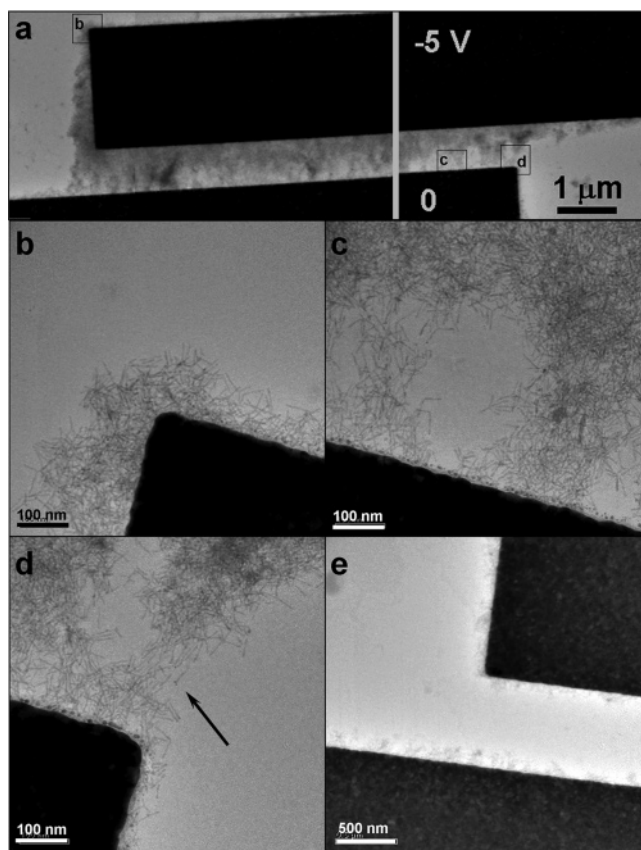
ImageJ software to obtain the value of  $\theta$  for each NR (see also Supporting Information Figures S1 and S2).

Figure 4a is a histogram showing the distribution of  $\theta$  values for four different electrode gaps where CdSe NRs were drop cast from solutions with  $\sim 10^{12}$  to  $\sim 10^{13}$  rods/mL. Analysis of hundreds of CdSe and CdTe NRs gave an average value of  $S \approx 0.8$  for field strengths of  $E \approx 2 \times 10^7$  V/m and  $S \approx 0.1$  for zero field (Figure 4b). A simple consideration of thermal energy allows an estimate of the lower bound of the electric dipole magnitude. Assuming both a permanent dipole moment,  $d_0$ , and an induced dipole moment,  $d_1$ , characterized by a polarizability,  $\alpha$ , gives a total alignment energy  $U_{\text{align}} = E(d_0 + d_1)$  for an applied field,  $E$ . In order for strong NR alignment to be possible,  $U_{\text{align}}$  must be greater than the thermal energy at room temperature,  $k_B T = 26$  meV ( $k_B$  is the Boltzmann constant). On the basis of TEM image analysis, we estimated the minimum field necessary for significant alignment to be  $E_{\text{min}} \approx 2 \times 10^7$  V/m and therefore the total dipole moment,  $d_0 + d_1$ , must be at least 300 D. This estimate is consistent with the previous measurements reporting  $d_0 \approx 200$  D<sup>15</sup> and  $\alpha \approx 10^{-25}$  m<sup>3</sup>,<sup>19</sup> which for  $E = 2 \times 10^7$  V/m corresponds to  $d_1 \approx 100$  D.

In addition to NR alignment, Figure 3 suggests that the electric field forces a higher concentration of NRs inside the gap than in the surrounding regions outside. To further probe this accumulation effect, we explored even higher concentra-

tions of NRs ( $\sim 10^{14}$  rods/mL). Figure 5 is a TEM image showing a clear example of the electric-field-driven accumulation for CdSe NRs deposited with the electrodes oppositely biased at  $\pm 8$  V. In this case, CdSe NRs are densely accumulated inside of the 270 nm  $\times$  1  $\mu\text{m}$  gap and the NR concentration falls off rapidly outside. In fact, the edge of the NR region outside the gap has the same shape as the electric field contours that one would expect for this device geometry. Parts b and c of Figure 5 are simulations (Maxwell 2D software) of the electric field contours for the device parameters in this example. This gap was situated between two floating electrode pairs, as is indicated in the simulation. Indeed, the electric field contours strongly resemble the concentration contours seen in the TEM image (compare parts a and b of Figure 5) and NRs along the edges are oriented in the direction of the field. This robust accumulation effect was seen for all devices (cf. Supporting Information Figure S4). The higher concentration of NRs leads to multiple layers and it is therefore difficult to quantify the degree of alignment from the TEM images.

Figure 6 shows TEM images of a device ( $L = 400$  nm,  $W = 15$   $\mu\text{m}$ ) where only the upper electrode was voltage-biased ( $-5$  V) during deposition and the lower electrode was grounded. CdTe NRs were deposited from solution at  $\sim 10^{13}$  rods/mL. Though the gap is seen to be nearly filled, the NRs clearly prefer the upper electrode. Additionally, some degree of alignment is observable in the more dilute areas (Figure



**Figure 6.** TEM images of an electrode gap ( $L = 400$  nm,  $W = 15$   $\mu\text{m}$ ) after deposition of CdTe NRs ( $\sim 10^{13}$  rods/mL) applying  $-5$  V to the upper electrode and grounding the other (i.e.,  $E = 6.3 \times 10^6$  V/m). (a) Overview image of NR accumulation in the gap. The gap section not shown (middle,  $\sim 8$   $\mu\text{m}$  wide), shows a similar NR distribution. (b–d) Higher magnification TEM images of different regions of a at the indicated locations. Some degree of alignment can be observed in the dilute regions close to the edge (arrow). All scale bars = 100 nm. (e) TEM image of an adjacent gap region, which was “floating” (i.e.,  $E = 0$ ) during the NR deposition, showing almost no NRs in the gap.

6d). These results were observed for both positive and negative voltage bias. The accumulation effect is never observed for unbiased gaps, even if they are on the same membrane as biased gaps (cf. Figure 6e and Supporting Information Figure S3).

Finally, we explored deposition in the case of a relatively large gap ( $L = 1.1$   $\mu\text{m}$  and  $W = 500$  nm). Figure 7a shows TEM images of CdSe NRs deposited from solution at  $10^{14}$  rods/mL while the electrode was held at 9 V (the opposite electrode was grounded). The NRs accumulated roughly evenly around the perimeter of the electrode. As shown more closely in Figure 7b and c, the NRs in contact with the electrode are aligned perpendicular to its edge in the plane of the substrate; most notably at the electrode corners where the field is strongest.

To gain insight into the degree of accumulation in the  $z$  direction (i.e., out of the page), we performed height analysis with AFM. Figure 8 shows an AFM height image of the same device shown in Figure 7. The top left electrode (“1T”) was biased (9 V) at the time of NR deposition, while the bottom left electrode (“1B”) was grounded and the others

were left floating. Inspection of the line scan labeled “I” (Figure 8, top inset) reveals that electrode “1T” is  $\sim 60$  nm higher than “2T.” This additional height corresponds to either  $\sim 18$  monolayers (MLs) of NRs if their long axis are parallel to the electrode surface (i.e., “lying down”),  $\sim 2$  MLs if they are perpendicular (i.e., “standing up”), or a combination of both, though the two orientations cannot be distinguished by AFM. From line scan “II,” the region inside the gap is seen to be up to  $\sim 15$  nm higher than the membrane surface, which can correspond to  $\sim 4$  MLs lying down.

Figure 9 shows AFM images of another device ( $L = 400$  nm;  $W = 15$   $\mu\text{m}$ ) before (inset) and after deposition of CdTe NRs from a solution concentrated to  $\sim 10^{14}$  rods/mL. During deposition, a 5 V bias was applied to the electrode labeled “2R”, while “2L” was grounded. The other two gaps in the image were left floating. The postdeposition AFM height analysis revealed that “2R” is  $\sim 200$  nm higher than all other electrodes, corresponding to  $\sim 3$  MLs standing up or  $\sim 30$  MLs lying down. NR coverage is  $< 0.1$  ML in all other regions of the device including electrode “2L”, as determined from the difference between AFM images of the same locations taken before and after NR deposition.

There could be several contributing forces that drive the accumulation. A neutral object with a dipole moment (either permanent or induced) would experience a force that scales with the field gradient. This dielectrophoresis force may drive the NRs to the electrodes, where the field is the strongest, to maximize the polarization energy. Our field simulation gives a field magnitude  $|E| < 10^5$  V/m and field gradient magnitude  $|\nabla E| < 10^{11}$  V/m<sup>2</sup> at  $\sim 10$   $\mu\text{m}$  away from the biased electrodes. At this field strength, the induced dipole  $d_1 \approx 1$  D  $\ll$  the permanent dipole  $d_0 \approx 200$  D.<sup>15,19</sup> The dielectrophoretic force  $\nabla(d_0 E + d_1 E)$  is therefore dominated by the permanent dipole moment  $d_0$ . It will take a NR a time of  $10^4$  s to migrate 1  $\mu\text{m}$ , when  $\sim 10$   $\mu\text{m}$  away from the biased electrode, a rather slow process. The fact that the robust accumulation of CdSe and CdTe NRs occurs even when the electric fields were applied for as little as 10 min indicates that the NRs migrate rapidly to the biased electrodes. Another possible explanation for the migration is the electrophoresis force, if the NRs have net charges. In fact, charge on NCs have been reported.<sup>3,8,14</sup> Assuming only one electron charge on each NR, at  $\sim 10$   $\mu\text{m}$  away from the biased electrodes, the electrophoretic force  $qE > 100$  times the dielectrophoretic force. A permanent charge therefore corresponds to a significantly faster migration speed, consistent with the rapid accumulation that we observe. However, the NR dynamics are complicated by the nonequilibrium nature of the system due to fluid flow during the evaporation of the droplet and NRs could move faster than predictions based on assuming a static force field. Our experiment was designed to study NR assembly in an electric field during drop casting, and the accumulation results alone do not allow for a distinction between contributions from dielectrophoresis and electrophoresis.

In conclusion, we have observed alignment of well-isolated (noninteracting), as well as closely packed CdSe and CdTe NRs to the direction of an applied electric field and their

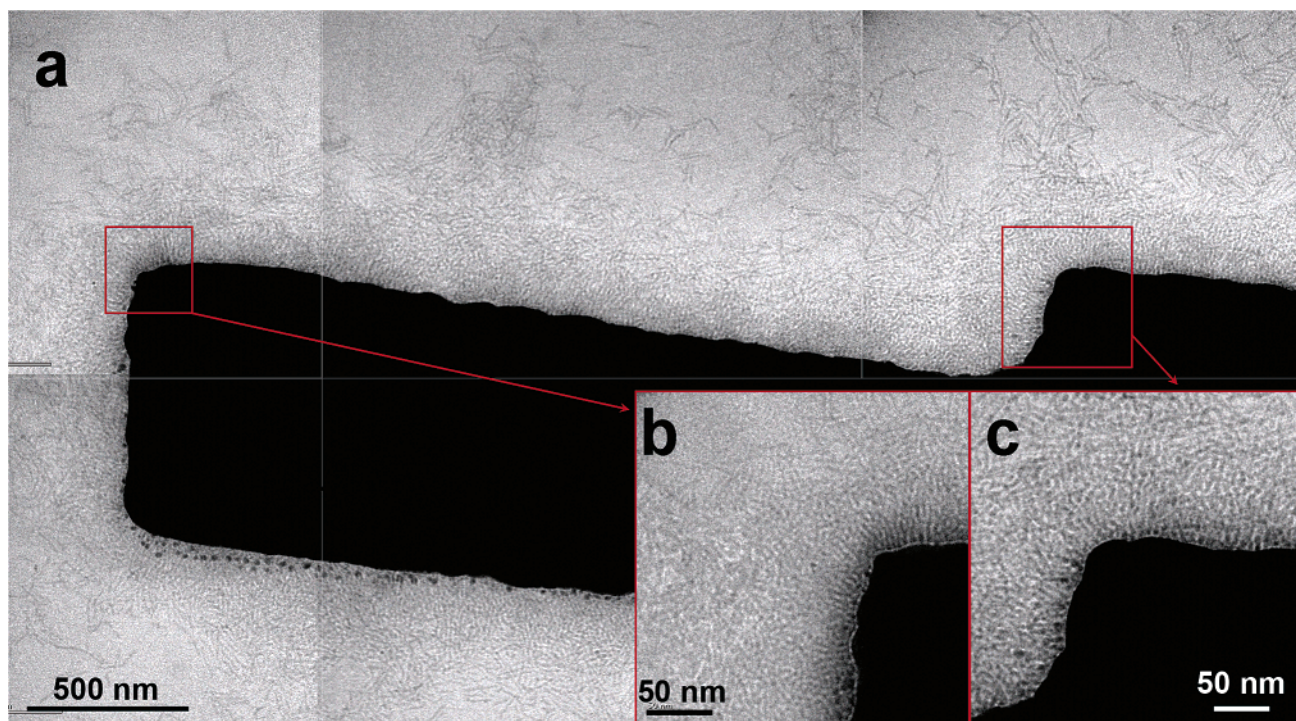


**Figure 7.** (a) TEM image (created by pasting together 5 images) showing accumulation of CdSe NRs around one electrode ( $L = 1.1 \mu\text{m}$ ,  $W = 500 \text{ nm}$ ) after deposition from a concentrated solution ( $\sim 10^{14}$  rods/mL) with the electrode at 9 V ( $E = 4.1 \times 10^6 \text{ V/m}$ ). (b and c) Higher magnification images of the two corners of the electrode that are marked with red boxes. The NRs closest to the electrode appear perpendicular to the electrode edge.

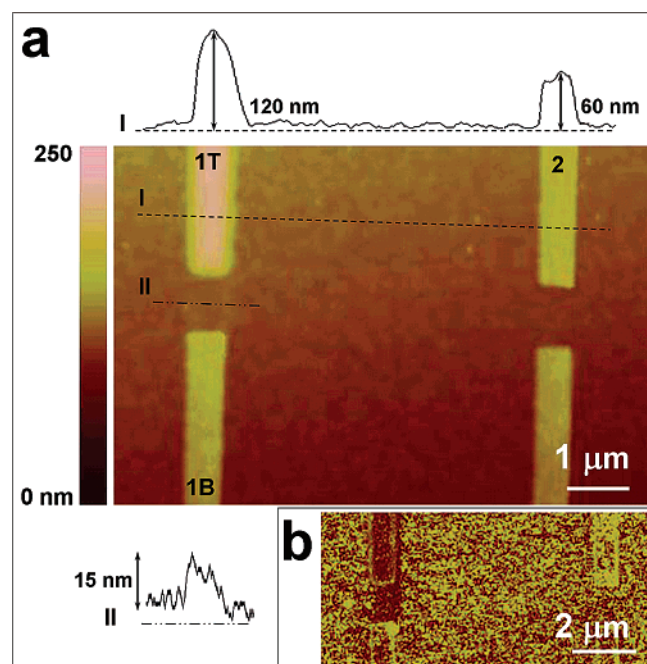


**Figure 8.** AFM image of an electrode gap ( $L = 1.1 \mu\text{m}$ ,  $W = 500 \text{ nm}$ ) after deposition of CdSe NRs with the electrode “1T” at 9 V and “1B” at 0 V. Electrode pair “2” was left “floating” ( $E = 4.1 \times 10^6 \text{ V/m}$ ). The electrode “1T” is the same electrode as in Figure 7. (a) Topographic image with the line scans I (top inset) and II (bottom inset) in two different regions. (b) Phase image of the same device, showing the accumulation of NRs onto “1T” and inside the gap.

accumulation onto voltage-biased electrodes and within nanoscale gaps. These results could be relevant for NR-based

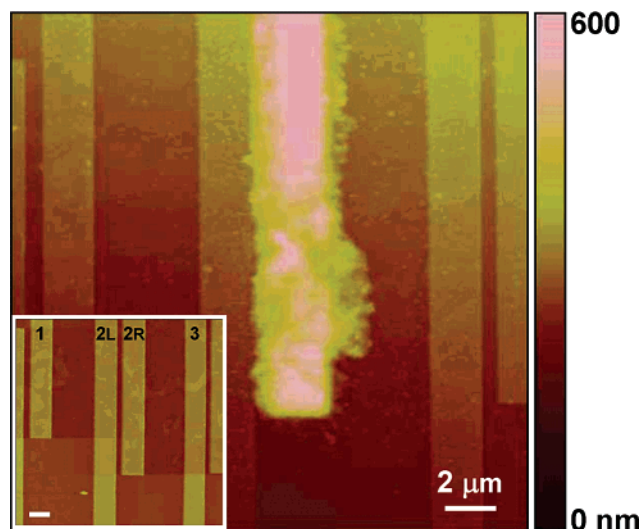


**Figure 9.** AFM topographic images of an electrode gap ( $L = 400 \text{ nm}$ ,  $W = 15 \mu\text{m}$ ) before (inset) and after deposition of CdTe NRs ( $\sim 10^{14}$  rods/mL) while applying 5 V to electrode “2R” and 0 V to “2L” (i.e.,  $E = 6.3 \times 10^6 \text{ V/m}$ ). The neighboring electrode pairs (“1” and “3”) were left “floating”. The scale bars =  $2 \mu\text{m}$ .

applications including light-emitting devices, optical sensors, switches, and solar cells. Electrodeposition provides a practical method to place NRs at desired positions on a chip and align them in preferred directions. We have also observed the accumulation effect with branched CdTe nanostructures (Supporting Information Figure S5). In addition to the technological potential for this robust spatial control, these results are evidence of the existence of induced and/or permanent electric dipole moment in semiconducting NRs.

**Acknowledgment.** We thank D. Tran and S. Wang for experimental assistance. This work has been funded by, NSF Career Award DMR-0449533, NSF MRSEC DMR05-20020, NSF NSEC DMR-0425780, and ONR awards YIP-N000140410489 and N000140510393. M.F. acknowledges funding from the NSF-IGERT program (Grant DGE-0221664).

**Supporting Information Available:** Additional TEM images of electrodeposited CdSe and CdTe NRs and details of the statistical analysis of the alignment. This material is available free of charge via the Internet at <http://pubs.acs.org>.

## References

- (1) Peng, X. G.; Manna, L.; Yang, W. D.; Wickham, J.; Scher, E.; Kadavanich, A.; Alivisatos, A. P. *Nature* **2000**, *404*, 59–61.
- (2) Murray, C. B.; Kagan, C. R.; Bawendi, M. G. *Annu. Rev. Mater. Sci.* **2000**, *30*, 545–610.
- (3) Shevchenko, E. V.; Talapin, D. V.; Kotov, N. A.; O'Brien, S.; Murray, C. B. *Nature* **2006**, *439*, 55–59.
- (4) Lin, X. M.; Jaeger, H. M.; Sorensen, C. M.; Klabunde, K. J. *J. Phys. Chem. B* **2001**, *105*, 3353–3357.
- (5) Talapin, D. V.; Shevchenko, E. V.; Murray, C. B.; Kornowski, A.; Förster, S.; Weller, H. *J. Am. Chem. Soc.* **2004**, *126*, 12984–12988.
- (6) Li, L. S.; Alivisatos, A. P. *Adv. Mater.* **2003**, *15*, 408–411.
- (7) Bezryadin, A.; Dekker, C.; Schmid, G. *Appl. Phys. Lett.* **1997**, *71*, 1273–1275.
- (8) Islam, M. A.; Herman, I. P. *Appl. Phys. Lett.* **2002**, *80*, 3823–3825.
- (9) Cui, Y.; Bjork, M. T.; Liddle, J. A.; Sonnichsen, C.; Boussert, B.; Alivisatos, A. P. *Nano Lett.* **2004**, *4*, 1093–1098.
- (10) Hu, J.; Li, L.-S.; Yang, W.; Manna, L.; Wang, L.-W.; Alivisatos, A. P. *Science* **2001**, *292*, 2060–2063.
- (11) Ryan, K. M.; Mastroianni, A.; Stancil, K. A.; Liu, H.; Alivisatos, A. P. *Nano Lett.* **2006**, *6*, 1479–1482.
- (12) Gupta, S.; Zhang, Q.; Emrick, T.; Russell, T. P. *Nano Lett.* **2006**, *6*, 2066–2069.
- (13) Ghezelbash, A.; Koo, B.; Korgel, B. A. *Nano Lett.* **2006**, *6*, 1832–1836.
- (14) Krishnan, R.; Hahn, M. A.; Yu, Z.; Silcox, J.; Fauchet, P. M.; Krauss, T. D. *Phys. Rev. Lett.* **2004**, *92*, 216803.
- (15) Li, L. S.; Alivisatos, A. P. *Phys. Rev. Lett.* **2003**, *90*, 097402.
- (16) Fischbein, M. D.; Drndic, M. *Appl. Phys. Lett.* **2006**, *88*, 063116.
- (17) In brief, 3.4 nm × 38 nm CdSe NRs were prepared by injecting slowly (over ~1 min) four times 0.2 mL of a 1.0 M TOPSe solution every 5 min at 255 °C into a solution containing 50 mg CdO, 150 mg DPA, and 2.9 g TOPO, previously degassed for 1 h at 300 °C. After a reaction time of 20 min, the nanorods were precipitated and washed with methanol. 6 nm × 50 nm TOPO-capped CdTe NRs were synthesized by the same method, using 40 mg CdO, 140 mg DPA, and 2.5 g TOPO. 4 × 0.2 mL of 0.1 M TOPTe were injected at 300 °C every 2 min (total reaction time 8 min).
- (18) Shieh, F.; Saunders, A. E.; Korgel, B. A. *J. Phys. Chem. B* **2005**, *109*, 8538–8542.
- (19) Empedocles, S. A.; Bawendi, M. G. *Science* **1997**, *278*, 2114–2117.

NL0620379